Translational diffusion of water and its dependence on temperature in charged and uncharged clays: a neutron scattering study. J. Chem. Phys. 129, 174706–174716

ARTICLE *in* THE JOURNAL OF CHEMICAL PHYSICS · DECEMBER 2008

Impact Factor: 2.95 · DOI: 10.1063/1.3000638 · Source: PubMed

Applied Geochemistry 23 (2008) 3840–3851

Contents lists available at ScienceDirect

Applied Geochemistry

journal homepage: www.elsevier.com/locate/apgeochem

Review

Self-diffusion of water and its dependence on temperature and ionic strength in highly compacted montmorillonite, illite and kaolinite

Fátima González Sánchez [a,*,1], Luc R. Van Loon [a], Thomas Gimmi [a,b], Andreas Jakob [a], Martin A. Glaus [a], Larryn W. Diamond [b]

[a] Laboratory for Waste Management, Paul Scherrer Institute, CH-5232 Villigen PSI, Switzerland
[b] Institute of Geological Sciences, University of Bern, CH-3012 Bern, Switzerland

ARTICLE INFO

Article history:
Received 19 March 2008
Accepted 9 August 2008
Available online 15 August 2008

Editorial handling by R. Fuge

ABSTRACT

The effect of temperature and ionic strength on the diffusion of HTO parallel to the direction of compaction through 5 highly compacted clay minerals (bulk dry density, $\rho_{b,d}$ = 1.90 ± 0.05 Mg/m^3), namely montmorillonite (Na- and Ca-form), illite (Na- and Ca-form), and kaolinite, was studied. The diffusion experiments were carried out at temperatures between 0 °C and 60 °C and at ionic strengths of 0.01 M and 1 M NaCl for the Na-form clays and kaolinite, and of 0.005 M and 0.5 M $CaCl_2$ for the Ca-form. The ionic strength had an insignificant influence on the values of the effective diffusion coefficient (variation by less than 10%) for the clays under study at this degree of compaction. The effective diffusion coefficients followed the order Na-montmorillonite < Ca-montmorillonite < Ca-illite < Na-illite ⩽ kaolinite. It is thought that the differences between Na- and Ca-montmorillonite originate from the larger size particles, and thus the lower tortuosity of the latter; whereas the differences between Na- and Ca-illite are related to the different degree of solvation of the Na and Ca cations. The activation energies were successfully calculated using the Arrhenius law. Swelling clays (Na- and Ca-montmorillonite) had slightly larger activation energy values (20 kJ/mol) compared to bulk water (17 kJ/mol); Ca-illite (16 kJ/mol), Na-illite (13 kJ/mol) and kaolinite (14.4 kJ/mol) lower values than that of bulk water. The low activation energies of the last three clays may be related to weaker H-bonds between water and the clay surfaces compared to those in bulk water.

Contents

* Corresponding author. Tel.: +41 765054129; fax: +41 563103565.
E-mail address: fatima_oti@yahoo.com (F. González Sánchez).
[1] Present address: Mehrhaldenstrasse 8, CH-5415 Nussbaumen, Switzerland.

0883-2927/$ - see front matter © 2008 Elsevier Ltd. All rights reserved.
doi:10.1016/j.apgeochem.2008.08.008

1. Introduction

Compacted clays and shales are impermeable and therefore effective barriers to fluid flow in near-surface groundwater environments and in deep sedimentary basins. Owing to their impermeability and their sorption properties, compacted clay formations have been proposed as host rocks for deep underground repositories of radioactive waste. Furthermore, swelling clays like bentonite are the favored artificial sealing material for such repositories. Water dynamics in clays is dominated by the physicochemical interactions between water molecules and clay particles, and by the geometrical arrangement of the clay particles. The clay mineral-water system has to be well characterized to understand the migration of radionuclides or other solutes, which in these highly compacted and sorbing materials occurs predominantly by diffusion through the pore water.

The effective diffusion coefficient in a porous material can be related to the bulk water diffusion coefficient through various factors accounting for the decreased cross section available for diffusion (porosity), for geometric effects of the pore network (tortuosity and geometric constrictivity), for an increased viscosity of the pore solution, and for electrostatic constrictions (e.g. Li and Gregory, 1974; van Brakel and Heertjes, 1974; Boving and Grathwohl, 2001; Flury and Gimmi 2002; Bourg et al., 2006). Because the different factors cannot often be determined independently, the following relationship is used in this paper:

$$D_e = \frac{\varepsilon}{G} \cdot D_w, \quad (1)$$

where D_e (m^2/s) is the effective diffusion coefficient in the material defined per total cross section, ε [–] the porosity, D_w the bulk water diffusion coefficient (m^2/s), and G a factor accounting for geometric and all other restrictions. Note that here diffusion is considered at a length scale of centimeters; that is, at a scale much larger than the pore size.

The geometrical arrangement of the clay particles and thus the organization of the water molecules within the clay are directly related to the degree of compaction (Djeran-Maigre et al., 1998). The porosity and the pore size are reduced with increasing compaction (Vasseur et al., 1995) and the water is differently distributed. For instance in Na- and Ca-montmorillonite at bulk dry densities larger than 1.9 Mg/m^3, most of the water (>95%) is located in the lattice interlayers (Pusch, 2001). As a consequence, the effective diffusion coefficients decrease with increasing degree of compaction; i.e., bulk dry density (García-Gutiérrez et al., 2004). The type of interlayer cation, mainly because of the differences in charge, size and hydration energy, can directly affect the swelling behavior in clays (McBride, 1994; Ohtaki and Radnai, 1993), and therefore probably also its diffusion properties. For montmorillonite, the Ca-form has a larger d-spacing (Wu et al., 1997), a higher aggregate porosity and larger pore sizes than the Na-form. Hence, water in Ca-montmorillonite has higher diffusion coefficients (Choi and Oscarson, 1996) for the same degree of compaction.

The temperature dependence of rates of activated processes like chemical reactions can generally be described by the empirical Arrhenius equation. For diffusion, the following equation is in general used:

$$D_e = A \cdot e^{-E_a/RT}, \quad (2)$$

where A is the so-called pre-exponential factor, $R = 8.314$ J/(K mol) the molar gas constant, and E_a (kJ/mol) the activation energy. The activation energy represents the minimum amount of energy that is required to activate atoms or molecules to a condition in which they can undergo chemical transformations or physical transport. Activation energies are thought to give additional information on the microscopic processes that affect diffusion. Kozaki et al. (1998) found increasing activation energies for Na^+ tracer diffusion in Na-montmorillonite with increasing bulk dry density. Both Na- and Ca-montmorillonite show this effect (Kozaki et al., 2005), with activation energies of 14.1 ± 1.2 and 17.4 ± 1.6 kJ/mol, respectively, at a degree of compaction of 1 Mg/m^3 and 24.7 ± 1.5 and 24.4 ± 3.1 kJ/mol, respectively, at 1.8 Mg/m^3. For HTO diffusion in Na-montmorillonite at different degrees of compaction between 1.0 and 2.0 Mg/m^3, however, approximately constant values of about 18 ± 2 kJ/mol (Nakazawa et al., 1999; Suzuki et al., 2004) were found, which are not significantly different from that of bulk water self-diffusion (16 kJ/mol; Low, 1962; to 18 kJ/mol; Wang, 1951). In aqueous solutions the presence of kosmotrope ions (order-makers), such as Na^+ and Ca^{2+} (Hribar et al., 2002), increases the water activation energy for diffusion (Dill et al., 2005). This is because these ions exhibit stronger interactions with water molecules than water with itself. In clays, however, the character of the cations and their effect on water diffusion or activation energy is not yet clear (Gast, 1962; Oster and Low, 1963).

Only a few studies have compared water diffusion through different clays (swelling and non-swelling) at the same degree of compaction or at the same porosities. Such a comparison may be helpful when trying to interpret the relationship between clay structure and diffusion properties. Most of the literature focuses on specific swelling clays like bentonite or montmorillonite. Little is known, however, about diffusion through kaolinite (Phillips and Brown, 1968), and even less about diffusion through illite (Ellis et al., 1970). For instance, the authors are unaware of any study of the temperature dependence of diffusion through illite or kaolinite. There is also a lack of information about diffusion in compacted clays at different ionic

strengths. In the case of bulk water, the self-diffusion coefficient decreases when the concentration of NaCl increases, but increases with increasing KI concentration (Wang, 1954). In the case of clays, the ionic strength of the pore water can additionally have an effect on the microstructural organization of the solid particles (Wang and Siu, 2006), and thus on water transport in clays.

In this paper the dynamics of water are investigated in terms of the macroscopic diffusion coefficients in 5 pure, different natural clays in a compacted state ($\rho_{b,d}$ = 1.90 ± 0.05 Mg/m^3). The homogeneity of their mineralogical composition should simplify the study and the interpretation of the dynamics of water within the clay-rock systems. A one-dimensional through-diffusion method was applied, using both transient and steady state data. The values for the effective diffusion coefficients were obtained by taking into account the effect of the filter plates at the clay interfaces. It has been shown that this effect is important in the modelling (Melkior et al. 2005; Sato, 2002), and that one should even distinguish between unused filters and those having been in contact with compacted clays (Glaus et al., 2007). The diffusion coefficients were evaluated for different salt concentrations to test the effect of the ionic strength, for different cation forms (Na- and Ca- for montmorillonite and illite), and at different temperatures (0–60 °C) to obtain the activation energy of the diffusion process. Consequently, this study presents a comparison of water dynamics in highly compacted clays showing significant chemical and structural (fabric) differences.

2. Materials

Clays are layer silicate minerals composed of tetrahedral (T:Si tetrahedra) and octahedral (O:Al octahedra) sheets. Two or three such sheets form a TO or TOT layer. Several sequences of these layers are combined and form larger units called stacks. Several clay stacks combine to produce particles and aggregates.

The clay mineral group is defined by the type of combination of sheets to layers, and the type of interlayers that hold the layers together. Montmorillonite and illite are formed by TOT layers. In these two groups of clays isomorphic substitutions (i.e., replacement of ions in the crystals without change of the structure) result in a net negative charge, which is balanced through the electrostatic adsorption of cations in the interlayer space and cations on or near the external surfaces. Kaolinite is formed by TO layers and isomorphic substitution is rather small. Depending on their structure, type of interlayer cation, activity of water and the degree of compaction, clays can be hydrated by a variable amount of water molecules in the interlayer space and on external surfaces. In the case of montmorillonite, water is located in between particles and in the interlayer space. However, in illite water is only located in between particles, because the interlayer surfaces are tightly linked by K cations. Kaolinite has no interlayers, therefore water is located on the external surfaces (Fig. 1).

The clays studied were montmorillonite from Milos (Decher, 1997), illite du Puy (Gabis, 1958), both conditioned to the homoionic Na- and Ca-form, as well as kaolinite from

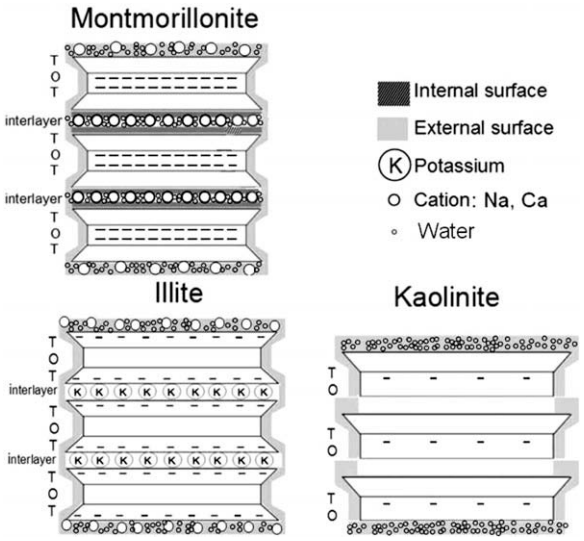

Fig. 1. Schematic representation of the structures of the clays used in this work. The small horizontal lines denote the negative charges present in the clay systems.

Georgia (KGa-2; van Olphen and Fripiat, 1979). The conditioning was performed by shaking the montmorillonite and illite clay powders for 3 h in a 1 M solution of NaCl or, for the Ca-form, of $CaCl_2$. After sedimentation the supernatant was decanted, and the procedure was repeated twice again. Afterwards, the clay was placed in dialysis bags and washed with Milli-Q water until the solution was free of Cl^- according to the $AgNO_3$ test (Slowinski et al., 2004). Finally, the Na- or Ca-conditioned clay was freeze dried (Mellor, 1978). Cylindrical pellets of 2.55 ± 0.01 cm in diameter, 1.00 ± 0.05 cm thickness, and a bulk dry density of 1.90 ± 0.05 Mg/m^3 were prepared from the freeze dried powder. The high degree of compaction was selected to reduce the pore size and increase the relative water–clay interface.

The transport and diffusion properties of a pellet depend strongly on the clay structure; that is, on the arrangement of the clay particles and the water phase (Van Loon et al., 2004). In order to obtain a good picture on the specific distribution of water in the different clay samples, various properties of the clay powder and the pellets were determined.

Table 1 shows the results of the analyses of the powder state. The chemical composition of the clays was measured by inductively coupled plasma atomic emission spectroscopy (ICP-AES) analyses after fuming with $LiBO_2$ and dissolving the melt with HNO_3. From the chemical composition the approximate structural formulae of the clays were obtained. Particle size, obtained by SEM and dynamic light scattering experiments (zeta-sizer 5000, Malvern Instruments, Malvern, UK), external surface area (N_2 BET method) and total surface area (ethylene glycol monoethyl ether (EGME) method) are also reported in Table 1. For kaolinite, clay without interlayer space, the EGME surface was not measured because it was reported to be similar to the BET surface (Chorover et al., 1999).

The data given in Table 2 refers to the analyses of the clays in the compacted pellet state ($\rho_{b,d}$ = 1.9 Mg/m^3).

Table 1
Clay characterization of the powdered material

Part.size (μm)	BET (m^2/g)	EGME (m^2/g)
Na-montmorillonite: $[(Si_{3.93}Al_{0.07})\ O_{10}\ (OH)_2]\ (Al_{1.41}Fe_{0.09}Mg_{0.344})(Ca_{0.022}Na_{0.325}K_{0.044})$		
0.5	28.4	705
Ca-montmorillonite: $[(Si_{3.83}Al_{0.17})\ O_{10}\ (OH)_2]\ (Al_{1.33}Fe_{0.09}Mg_{0.34})(Ca_{0.22}Na_{0.025}K_{0.044})$		
1.1	38.3	707
Na-illite: $[(Si_{3.48}Al_{0.52})\ O_{10}\ (OH)_2]\ (Al_{1.18}Fe_{0.36}Mg_{0.39})(Ca_{0.054}Na_{0.11}K_{0.69})$		
0.32	112.0	111
Ca-illite: $[(Si_{3.46}Al_{0.54})\ O_{10}\ (OH)_2]\ (Al_{1.17}Fe_{0.36}Mg_{0.39})(Ca_{0.1}Na_{0.024}K_{0.7})$		
0.34	117.7	116
Kaolinite: $[(Si_4)\ O_{10}\ (OH)_4]\ (Al_{1.96}Fe_{0.039}Mg_{0.001})$		
1.3	45.8	–

Table 2
Clay characterization of the compacted pellet material

	N°particles/stack	*d*-Spacing (Å) (wet/dry)	ρ_s (Mg/m^3)	Porosity ε (%)	Water content (g/g)	Water layers
Na-montmorillonite	~3–5[a]	14.66/12.31	2.9 ± 0.1	32 ± 0.01	0.165 ± 0.005	~2
Ca-montmorillonite	~10–15[a]	15.82/14.32	2.8 ± 0.1	30 ± 0.01	0.155 ± 0.005	~2
Na-illite	~20–30[b]	9.92/9.88	2.7 ± 0.1	28 ± 0.01	0.145 ± 0.005	~9
Ca-illite	~20–30[b]	10.17/10.11	2.8 ± 0.1	30 ± 0.01	0.155 ± 0.005	~9
Kaolinite	~60[c]	7.16/7.16	2.6 ± 0.1	26 ± 0.01	0.135 ± 0.005	~20

[a] After Pusch (2001).
[b] After Poinssot et al. (1999).
[c] After Hassan et al. (2006).

The number of layers that form a stack are reported as found in the literature, whereas the other data in Table 2 were obtained in this study. The basal spacing was measured by XRD in a water-saturated and a dry state (110 °C, 24 h). The porosity, ε [–], was calculated from the solid density ρ_s (Mg/m^3), obtained by pycnometer measurements; and the bulk dry density $\rho_{b,d}$ (Mg/m^3) estimated from the mass of dry solid and the total volume of the sample, according to the relationship:

$$\epsilon = 1 - (\rho_{b,d}/\rho_s). \tag{3}$$

The water content is expressed in a gravimetric form as obtained from the amount of water added. Finally, the last column shows the average number of water layers between two clay surfaces, which were calculated as follows:

$$\text{Layers}_{\text{water}}\ [-] = \frac{2 \cdot w}{S_{\text{EGME}} \cdot \rho_w \cdot \phi_w}, \tag{4}$$

with w (g_{water}/g_{solid}) the gravimetric water content, S_{EGME} (m^2/g) the total surface area, ρ_w (Mg/m^3) the water density assumed to be 1 Mg/m^3, and ϕ_w = 0.3 nm the diameter of a water molecule. This calculation makes no assumption regarding particle size, shape or orientation, but assumes that the water films are equally spread over all surfaces. Consequently these values must be considered as the average number of water layers between two clay particle surfaces. Note that in the case of the swelling clays at the given density, most of this water is located in interlayers, whereas in the case of non-swelling clays it is located between external surfaces.

3. Methods

The clay powder was compacted within the diffusion-cell and confined between two filter plates. The cell was connected on each side to a reservoir, and the solution on each side was circulated using a peristaltic pump. Both compartments were filled with solutions of high or low ionic strengths (1 M or 0.01 M NaCl and 0.5 M or 0.005 M $CaCl_2$). One reservoir had a volume of $2 \times 10^{-3}\ m^3$, whereas the other had a volume of $3 \times 10^{-5}\ m^3$. As a first step the samples were completely saturated over 4–5 weeks with salt solutions of a given ionic strength. The saturation of the samples was checked by weighing. Subsequently, the $2 \times 10^{-3}\ m^3$, bottle was spiked with tritiated water (HTO) having a concentration of $(1.870 \pm 0.028) \times 10^{-7}\ mol/m^3$, which essentially remained constant during the experiment.

The concentration gradient between the two reservoirs led to transport of the tracer from the labeled to the non-labeled reservoir. After certain time intervals (2–3 days) the solution in the small reservoir was replaced to maintain the tracer concentration essentially at zero.

By monitoring the amount of tracer transported from the spiked to the non-spiked container, it is possible to follow the transient and the steady phase of the diffusion of the tracer. The experiments at different temperatures were carried out using the continuous method (Van Loon et al., 2005). Starting from an initial temperature of 0 °C, the temperature was increased in steps of 10 °C, once a steady flux was achieved, up to a maximum temperature of 60 °C.

The activity $A^{\Delta t}$ (mol) of ^3H in a sample obtained during a time interval Δt (s) was calculated as:

$$A^{\Delta t} = \frac{N^{\Delta t}}{60 \cdot f}, \tag{5}$$

where $N^{\Delta t}$ are the measured counts/min, and f is the counting efficiency in counts/min/mol. The experimental average flux, j_{exp} ($mol/m^2\ s$), over the time interval Δt was then calculated as (Van Loon et al., 2003):

$$J_{\mathrm{exp}} = \frac{A^{\Delta t}}{S \cdot \Delta t} \tag{6}$$

where $S(\mathrm{m}^2)$ is the sample cross-sectional area for diffusion.

Molecular diffusion was assumed to be the prominent transport mechanism for the migration of HTO in the experiments. This was verified using the following calculation. According to Darcy's law, the distance, x_{advec} [m], that an advective front would travel within the time t in the experiment is

$$x_{\mathrm{advec}} = \frac{v_{\mathrm{D}}}{\varepsilon} \cdot t = -K_{\mathrm{h}} \cdot \frac{\Delta h}{\Delta x} \cdot \frac{t}{\varepsilon} \tag{7}$$

Here v_{D} [m/s] is the Darcy's velocity. In the experimental system, the pressure difference Δh across the sample was always smaller than about 5–10 cm. For this pressure difference and a hydraulic conductivity, K_{h}, which varies depending on the type of clay and the degree of compaction between 10^{-14} and 10^{-12} m/s (Bucher and Spiegel, 1984; Pusch, 2001), a porosity ε of 0.3, a sample thickness Δx of 1 cm, and an experimental time t of 30 days, the distance travelled by the advective front would be only about 0.5 to 100 μm. Clearly, such a small effect can be neglected compared to transport by diffusion.

The clay sample was considered to be homogeneous regarding transport properties. A slight anisotropy of transport properties may result from the preparation of the samples, which were placed with the preferred orientation of their particles perpendicular to the direction of diffusion.

4. Modelling

The system to be solved is described by 3 transport domains in series, consisting of a filter $(0, x_1)$, the clay plug (x_1, x_2) and a second filter (x_2, L), (Fig. 2). Solving the equations for the 3-region system requires the values of the effective diffusion coefficients to be known. As shown by Glaus et al. (2007), the filter properties change from a fresh (unused) to a used state and also depend on the type of clay with which the filter was in contact. This was interpreted as the result of a partial clogging of the filter micropores by clay particles. The filter diffusion coefficients for used filters for HTO given in Table 3 for montmorillonite and kaolinite were calculated based on the ratios between used and fresh filters reported for ^{22}Na and ^{85}Sr tracers (Glaus et al., 2007). For illite, no measurements were available. Because illite is non-swelling, similar to kaolinite, it seems reasonable to assume the same ratio of reduction as for kaolinite. In fact a slightly larger value of 0.78 was used that is the average of a zero reduction and the reduction obtained for the swelling montmorillonite.

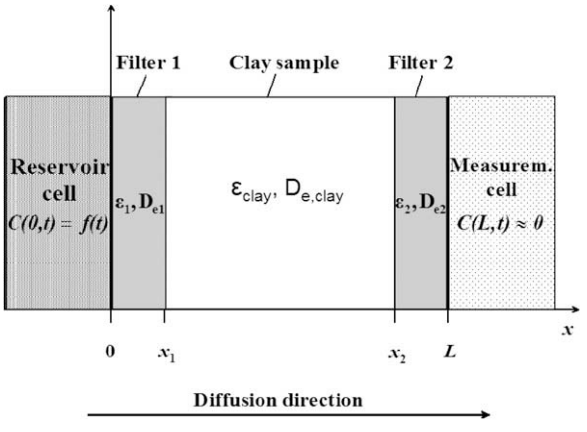

Fig. 2. A 2-dimensional sketch of the filter-clay-filter system used in the experiments.

Table 3
Filter effective diffusion coefficients for HTO in a fresh, $D_{\mathrm{f,fresh}}$, and used state for montmorillonite, $D_{\mathrm{f,mont}}$, and kaolinite, $D_{\mathrm{f,kao}}$

T (°C)	$D_{\mathrm{f,fresh}}$ (m^2/s)	$D_{\mathrm{f,mont}}$ (m^2/s)	$D_{\mathrm{f,kao}}$(m^2/s)
0	1.2×10^{-10}	6.9×10^{-11}	9.0×10^{-11}
10	1.6×10^{-10}	9.0×10^{-11}	1.2×10^{-10}
20	2.0×10^{-10}	1.1×10^{-10}	1.5×10^{-10}
25	2.3×10^{-10}	1.3×10^{-10}	1.7×10^{-10}
30	2.6×10^{-10}	1.4×10^{-10}	1.9×10^{-10}
40	3.2×10^{-10}	1.8×10^{-10}	2.3×10^{-10}
50	4.0×10^{-10}	2.2×10^{-10}	2.9×10^{-10}
60	4.7×10^{-10}	2.7×10^{-10}	3.5×10^{-10}

The different temperature values were obtained by Arrhenius law assuming an energy activation of 17 ± 1 kJ/mol (Low, 1962; Wang, 1951). The errors are estimated to be not larger than 10%.

The effective diffusion coefficients of the filters for the other temperatures given in Table 3 were calculated according to the Arrhenius law and using the activation energy of bulk water, i.e. 17 ± 1 kJ/mol (Low, 1962; Wang, 1951). The filter effect is relevant when the effective diffusion coefficients of the clay are in the same order of magnitude as those of the filter (case of kaolinite and illite for the experimental setup of a 1 cm sample thickness). However, this effect is not significant for clays with effective diffusion coefficients much smaller (one order of magnitude or more) than those of the filters, such as in case of montmorillonite.

Diffusion can be described by Fick's second law in one spatial dimension:

$$\frac{\partial C}{\partial t} = \frac{D_{\mathrm{e}}}{\alpha} \frac{\partial^2 C}{\partial x^2} \tag{8}$$

Here $D_{\mathrm{e}} = D_{\mathrm{p}} \cdot \varepsilon$, where D_{p} (m^2/s) is the pore diffusion coefficient; C (mol/m^3) is the tracer concentration in the mobile phase, x (m) the spatial coordinate, t (s) the time and α (–) the rock capacity factor defines as:

$$\alpha = \varepsilon + \rho_{\mathrm{b}} \cdot K_{\mathrm{d}} \tag{9}$$

with ρ_{b} (kg/m^3) the bulk dry density, and K_d (m^3/kg) the sorption distribution coefficient. For non-sorbing tracers such as HTO, $K_{\mathrm{d}} = 0$ and $\alpha = \varepsilon$. Eq. (8) applies for the clay sample, as well as the two filter regions.

A suitable initial condition to solve Eq. (8) is:

$$C(x, t \leqslant 0) = 0; \text{for all } x \in [0, L],$$

where L (m) is the total system thickness.

The boundary conditions are as follows:

1. $C(\{x = 0, t > 0\}) = C_0$
2. $C(\{x = L, t > 0\}) \approx 0$

The continuity conditions at the interfaces filter/clay are:

$$\left.\begin{aligned} C(x_{1-},t) &= C(x_{1+},t) \\ C(x_{2-},t) &= C(x_{2+},t) \end{aligned}\right\} \text{ for all } t > 0$$

$$\left.\begin{aligned} j(x_{1-},t) &= j(x_{1+},t) \\ j(x_{2-},t) &= j(x_{2+},t) \end{aligned}\right\} \text{ for all } t > 0$$

$$\text{with } \left.\begin{aligned} x_{1-,2-} &= x_{1,2} - \delta \\ x_{1+,2+} &= x_{1,2} + \delta \end{aligned}\right\} 1 >> \delta > 0$$

meaning that the concentration C and the flux j are continuous across the filter-clay interfaces.

The system of equations was solved using COMSOL Multiphysics V3.2b (www.comsol.com). The effective diffusion coefficient $D_{e,clay}$ was varied until the calculated flux according to Fick's first law,

$$J_{model} = -D_{e,2}\left.\frac{\partial C}{\partial x}\right|_{x=L}, \quad (10)$$

matched the experimental flux, j_{exp}, calculated by Eq. (6). The HTO effective diffusion coefficient $D_{e,clay}$ was obtained from the steady-state part of the flux vs. time curves. The clay porosity, ε_{clay}, was calculated from the transient part and then compared with that obtained from the density measurements. The fitting was done "by eye", that is, by a visual estimation of the goodness of the fit along with a careful scrutiny of its underlying parameter values.

Errors of the effective diffusion coefficients, D_e, were calculated based on first-order error propagation taking into account the error of the j_{exp} as calculated from the uncertainties of the quantities in Eq. (6), the thickness of the clay sample ($\Delta x_s = 0.001$ mm), the filter diffusion coefficient, D_f, and the concentration measurements, $\Delta C_0 = 2.8 \times 10^{-9}$ mol/m^3. In case of the porosity, ε, the same uncertainties were considered plus that of the breakthrough time t_{bt} (s) ($\Delta t_{bt} = 0.2$ days), which is the zero crossing of the regression line from the cumulative activity of the low concentration reservoir vs. time.

5. Results and discussion

5.1. Clay porosities and densities

Fig. 3 shows the quality of the fits for the flux curve vs. time for some of the studied clays at 0 °C. The clay porosities, ε_{clay}, calculated from the diffusion experiments were similar to those obtained from physical data ($\rho_{b,d}$ and ρ_s, the latter being measured by pycnometry; Table 2); but with a relatively high uncertainty (Tables 4–8). These results are presented here just for comparison purposes, because the porosities obtained from physical data (pycnometer measurements) are considered finally as more

Table 4
Na-montmorillonite: effective diffusion coefficients (m^2/s) at different temperatures and ionic strength

Na-montmorillonite T (°C)	1 M NaCl D_e (m^2/s)	0.01 M NaCl D_e (m^2/s)
0	$(6.89 \pm 0.70) \times 10^{-12}$	$(7.60 \pm 0.73) \times 10^{-12}$
10	$(9.80 \pm 0.90) \times 10^{-12}$	$(1.04 \pm 0.10) \times 10^{-11}$
20	$(1.35 \pm 0.12) \times 10^{-11}$	$(1.50 \pm 0.15) \times 10^{-11}$
30	$(1.79 \pm 0.18) \times 10^{-11}$	$(2.00 \pm 0.22) \times 10^{-11}$
40	$(2.41 \pm 0.25) \times 10^{-11}$	$(2.60 \pm 0.26) \times 10^{-11}$
50	$(3.00 \pm 0.31) \times 10^{-11}$	$(3.25 \pm 0.33) \times 10^{-11}$
60	$(3.62 \pm 0.35) \times 10^{-11}$	$(3.93 \pm 0.40) \times 10^{-11}$
70	$(4.58 \pm 0.46) \times 10^{-11}$	$(4.90 \pm 0.49) \times 10^{-11}$
$n°$ repetitions	2	2
ε	0.30 ± 0.12	0.32 ± 0.13
E_a(kJ/mol)	20.91 ± 0.42	20.78 ± 0.42

Porosity and activation energy values (kJ/mol) are also given.

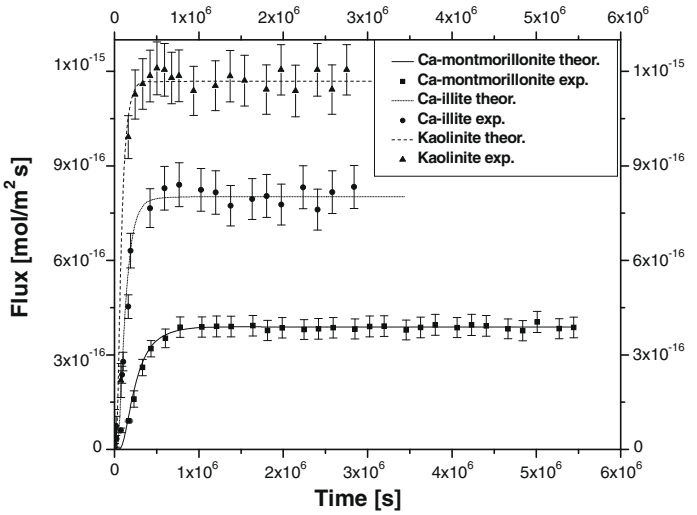

Fig. 3. Measured (symbols) and modeled (lines) fluxes vs. time for Ca-montmorillonite, Ca-illite (both at 0.005 M $CaCl_2$ and $T = 0$ °C), and kaolinite (at 0.01 M NaCl and $T = 0$ °C).

Table 5
Ca-montmorillonite: effective diffusion coefficients (m^2/s) at different temperatures and ionic strength

Ca-montmorillonite T (°C)	0.5 M $CaCl_2$ D_e (m^2/s)	0.005 M $CaCl_2$ D_e (m^2/s)
0	$(1.71 \pm 0.17) \times 10^{-11}$	$(1.93 \pm 0.20) \times 10^{-11}$
10	$(2.48 \pm 0.25) \times 10^{-11}$	$(2.74 \pm 0.28) \times 10^{-11}$
20	$(3.45 \pm 0.36) \times 10^{-11}$	$(3.74 \pm 0.38) \times 10^{-11}$
40	$(5.60 \pm 0.51) \times 10^{-11}$	$(6.24 \pm 0.61) \times 10^{-11}$
60	$(8.50 \pm 0.83) \times 10^{-11}$	$(8.83 \pm 0.89) \times 10^{-11}$
$n°$ repetitions	2	2
ε	0.27 ± 0.11	0.27 ± 0.07
E_a (kJ/mol)	20.01 ± 0.80	19.30 ± 0.82

Porosity and activation energy values (kJ/mol) are also given.

Table 6
Na-illite: effective diffusion coefficients (m^2/s) at different temperatures and ionic strength

Na-Illite T (°C)	1 M NaCl D_e (m^2/s)	0.01 M NaCl D_e (m^2/s)
0	$(8.88 \pm 1.21) \times 10^{-11}$	$(8.61 \pm 1.12) \times 10^{-11}$
10	$(1.14 \pm 0.15) \times 10^{-10}$	$(1.08 \pm 0.14) \times 10^{-10}$
20	$(1.35 \pm 0.18) \times 10^{-10}$	$(1.37 \pm 0.18) \times 10^{-10}$
40	$(1.90 \pm 0.26) \times 10^{-10}$	$(1.87 \pm 0.23) \times 10^{-10}$
60	$(2.45 \pm 0.30) \times 10^{-10}$	$(2.44 \pm 0.31) \times 10^{-10}$
$n°$ repetitions	2	2
ε	0.30 ± 0.13	0.28 ± 0.12
E_a (kJ/mol)	12.61 ± 0.54	13.05 ± 0.54

Porosity and activation energy values (kJ/mol) are also given.

Table 7
Ca-illite: effective diffusion coefficients (m^2/s) at different temperatures and ionic strength

Ca-Illite T (°C)	0.5 M $CaCl_2$ D_e (m^2/s)	0.005 M $CaCl_2$ D_e (m^2/s)
0	$(5.40 \pm 0.56) \times 10^{-11}$	$(5.75 \pm 0.53) \times 10^{-11}$
10	$(7.46 \pm 0.85) \times 10^{-11}$	$(7.55 \pm 0.73) \times 10^{-11}$
20	$(9.19 \pm 0.80) \times 10^{-11}$	$(9.41 \pm 0.09) \times 10^{-11}$
40	$(1.45 \pm 0.16) \times 10^{-10}$	$(1.42 \pm 0.10) \times 10^{-10}$
60	$(2.00 \pm 0.19) \times 10^{-10}$	$(2.10 \pm 0.22) \times 10^{-10}$
$n°$ Repetitions	2	2
ε	0.26 ± 0.11	0.27 ± 0.11
E_a (kJ/mol)	16.42 ± 0.20	16.08 ± 0.20

Porosity and activation energy values (kJ/mol) are also given.

reliable, and these were used to obtain the values of D_e. The porosities vary slightly for the different clays, even though bulk dry densities were about $\rho_{b,d} \sim 1.90\ Mg/m^3$ in all cases. This is mainly because of the different solid or densities, with higher values for the montmorillonite (ρ_s = 2.9 Mg/m^3). Accordingly, the porosity ε of the kaolinite sample is lowest with 0.26, and the porosities of illite and montmorillonite are between 0.28 and 0.32.

5.2. Effective diffusion coefficients at 20 °C

The results obtained for the clays at the two different salt concentrations are presented in Tables 4–8. For all the clays the effective diffusion coefficients at different ionic strengths did not differ significantly (the differences are within the estimated error bars). Classical models of diffusion in compacted clays are based on the double-layer theory (van Olphen, 1966) used to describe the distribution of cations between two particle surfaces. According to this theory the ionic strength should have an effect on the effective diffusion coefficient. However, in clays compacted to more than 1.5 Mg/m^3 with a narrow pore size distribution the double-layer theory is no longer valid, as stated by Marry and Turq (2003), and confirmed by the present measurements.

The effective diffusion coefficients, D_e, measured for the various clay types under study increase in the following order: Na-montmorillonite < Ca-montmorillonite < Ca-illite < Na-illite ⩽ kaolinite. When eliminating the slight differences in porosities and comparing the pore diffusion coefficients, D_p, the same sequence is obtained as for D_e. Sodium-illite and kaolinite exhibited similar diffusion behavior at this degree of compaction (Fig. 4). Kaolinite shows the largest D_e because it has the largest content of free pore water and because of the absence or rather small number of cations. Calcium-illite had diffusion coefficients between those of Na-illite or kaolinite and those of the montmorillonites, but being much closer to the first group of non-swelling clays. In the swelling clays, Na- and Ca-montmorillonite, the diffusion coefficients are reduced one order of magnitude compared with the non-swelling. The fine net of interlayer pores present in these clays leads to a large tortuosity and thus a low diffusion coefficient. Sodium-, Ca-illite and kaolinite do not have interlayers, which leads to a less tortuous path compared to montmorillonite.

Table 8
Kaolinite: effective diffusion coefficients (m^2/s) at different temperatures and ionic strength

Kaolinite T (°C)	1 M $NaClO_4$ D_e (m^2/s)	1 M NaCl D_e (m^2/s)	0.01 M NaCl D_e (m^2/s)	Water D_e (m^2/s)
0	$(1.00 \pm 0.12) \times 10^{-10}$	$(1.13 \pm 0.14) \times 10^{-10}$	$(8.00 \pm 0.89) \times 10^{-11}$	$(8.48 \pm 0.98) \times 10^{-11}$
10		$(1.48 \pm 0.19) \times 10^{-10}$	$(1.05 \pm 0.12) \times 10^{-10}$	$(1.10 \pm 0.13) \times 10^{-10}$
20	$(1.60 \pm 0.19) \times 10^{-10}$	$(1.85 \pm 0.23) \times 10^{-10}$	$(1.34 \pm 0.15) \times 10^{-10}$	$(1.33 \pm 0.15) \times 10^{-10}$
40	$(2.32 \pm 0.26) \times 10^{-10}$	$(2.45 \pm 0.27) \times 10^{-10}$	$(1.95 \pm 0.21) \times 10^{-10}$	$(2.00 \pm 0.22) \times 10^{-10}$
60	$(3.32 \pm 0.37) \times 10^{-10}$	$(3.23 \pm 0.35) \times 10^{-10}$	$(2.74 \pm 0.29) \times 10^{-10}$	$(2.75 \pm 0.31) \times 10^{-10}$
$n°$ Repetitions	1	2	2	2
ε	0.28 ± 0.12	0.30 ± 0.13	0.28 ± 0.16	0.27 ± 0.12
E_a (kJ/mol)	14.71 ± 0.32	12.90 ± 0.90	15.36 ± 0.46	14.78 ± 0.32

Porosity and activation energy values (kJ/mol) are also given.

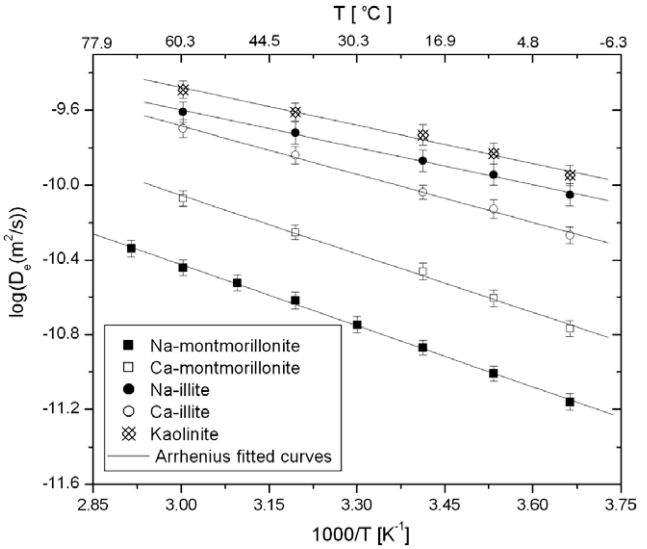

Fig. 4. Arrhenius plot: temperature dependence of the effective diffusion coefficients for different clay minerals at 1 M NaCl (Na- clay forms and kaolinite) and 0.5 M $CaCl_2$ (Ca-clay forms) ionic strengths.

In the following paragraphs, the results for each clay type will be discussed, with special emphasis on the effects of the cations.

The differences between **Na- and Ca-montmorillonites** are significant (Tables 4 and 5). The effective diffusion coefficients differ by about 60% (lower for the Na- than for the Ca-form). In particular samples of this study, Na- and Ca-montmorillonite pellets are hydrated on average with two layers of water (see Table 2), which agrees with the value given in the literature (Kozaki et al., 1998). Other studies (Fernández, 2003; Pusch, 2001) show that similar samples and at similar densities have > 95% of the total water content located in the interlayer space. Therefore, water in montmorillonite is mainly interlayer water, with the so-called external layer (water on external surfaces) and free pore water having a minor influence on the water diffusion parameters. The type of interlayer cation plays a dominant role in the interaction with water; and it also has an effect on the arrangement of the clay particles. This is attributed to the larger value for the effective diffusion coefficient found in Ca-montmorillonite compared to Na-montmorillonite mainly to the latter geometrical effect, which dominates over the direct cation-water interactions. Bivalent counterions between hydrophilic silica surfaces may generate an attractive force capable of maintaining larger stacks of silicate layers together (Marra, 1986). As a consequence, the average number of layers per stack or quasicrystal for Ca-montmorillonite is ~10–15, whereas in Na-montmorillonite it is only ~3–5 (Pusch, 2001). The particular way of stacking Ca-montmorillonite and the fact that the particle size is twice as large as that of the Na-form (Table 1), leads to a less "tortuous diffusion path" for water in the Ca- compared to the Na-montmorillonite. This is also confirmed by earlier Hg-intrusion porosimetry (Choi and Oscarson, 1996) with Ca-montmorillonite showing a greater proportion of relatively large pores than the Na-montmorillonite, and so a larger D_e. The chemical water-cation interaction seems to be less important. The fact that Ca has a higher hydration energy (−1660 kJ/mol) than the Na cation (−440 kJ/mol), which would make diffusion slower in the Ca- than in the Na-montmorillonite form, is possibly compensated by the twice as large number of monovalent Na ions as compared to bivalent Ca ions.

The most comparable results found in the literature are for Na-bentonite (Kunipia-F.) at a similar compaction of 1.8 Mg/m^3 (Kozaki et al., 1999) and with different particle sizes obtained by sieving. At 25 °C, they found D_e = $8.2{\cdot}10^{-11}$ m^2/s (particle size < 45 μm), and $7.3{\cdot}10^{-11}$ m^2/s (particle size of 75–150 μm) for diffusion of HTO when the clay was in contact with distilled water solutions. This value is higher than the value found in the present study at 20 °C, $D_e = (1.5 \pm 0.15) \times 10^{-11}$ m^2/s, or 30 °C, $D_e = (2.00 \pm 0.22) \times 10^{-11}$ m^2/s for HTO at the lowest ionic strength (0.01 M NaCl). There are several differences between the samples used by Kozaki et al. (1999) and those of the present experiments, which could explain this difference in results. Kozaki et al. (1999) used the Na-bentonite (Kunipia-F.) with a 95 wt.% montmorillonite content, whereas pure Na-montmorillonite from Milos was used in the present study. Because of the lower degree of compaction (1.8 Mg/m^3), the samples used by Kozaki et al. (1999) also had a larger porosity of 0.36 compared to those in the present study with a value of 0.32.

For **illite**, we calculated (Table 2) an average of 8 to 9 water layers between the clay particle surfaces was calculated (Table 2). Since only two water layers are strongly affected by the surfaces (Sposito and Prost, 1982) it is clear that for illite at this degree of compaction (or porosity) that the effective diffusion coefficients obtained are less influenced by the water located near the clay surfaces and more by the so-called free pore water, compared to montmorillonite. In the case of illite the two different cation forms (Na- and Ca-) have significantly different diffusion coefficients, with ca. 25% larger values for the Na-illite. In con-

trast to montmorillonite, it is thought that the differences in the effective diffusion coefficients for these two types of illite are mainly due to the differences in hydration or solvation of the Na and Ca cations. The size and arrangement of illite particles are mostly dominated by interaction with the K ions. Thus, the influence of the Na or Ca counterion on the geometry of the water path is expected to be irrelevant. Illite tends to build stacks formed by 20–30 TOT layers (Poinssot et al., 1999) in both the Na- and Ca-forms. The measurements also confirmed that both have similar particle size (Na-illite, 0.32 μm and Ca-illite 0.34 μm). The authors are not aware of similar experiments performed with illite, so cannot compare the results with those of other studies.

The water in **kaolinite** (films of 20 water layers were calculated, on average, between the clay particle surfaces) will be mainly free pore water. Only a small proportion (about 1–2 water-layers on each surface (Bridgeman and Skipper, 1997), or about 10–20% of the pore water in the kaolinite sample) will be affected by a particle surface. The samples studied were pre-saturated for approximately four weeks with four different solutions: water, 0.01 M NaCl, 1 M NaCl and 1 M $NaClO_4$. The differences between the diffusion coefficients measured in four different solutions are considered to be insignificant, but there is a tendency towards higher diffusion rates at high concentrations (Table 8). After observing no significant effect of ionic strength for the other clays, which potentially interact much more with water because of much larger accessible solid surfaces (Table 1, EGME and BET values), there is no reason to believe that in kaolinite at this density the effect should be more pronounced. The slight tendency observed could have two reasons. First, during the saturation process (4–5 weeks) with 1 M NaCl or 1 M $NaClO_4$, the previously inhomogeneously saturated kaolinite KGa-2 was probably transformed to its homoionic Na-form. This conditioning could slightly change the diffusion properties compared to the kaolinite saturated with 0.01 M NaCl, even though the CEC is only 3.3 meq/100 g (van Olphen and Fripiat, 1979). Second, as found elsewhere (Wang and Siu, 2006; Yong, 2003), a higher salt concentration appears to produce more face-to-face flocculation of the kaolinite particles, resulting in the formation of aggregates. This effect typically occurs in clays deposited under marine conditions. In the present case, kaolinite was first pressed into the pellet form, and then brought into contact with the different salt solutions. A slight reorganization of the particles could have occurred leading to a larger diffusion coefficients at high ionic strength.

Sachs et al. (2006) reported an effective diffusion coefficient of $D_e = (1.57 \pm 0.16) \times 10^{-10}$ m^2/s for water in kaolinite KGa-1 from Georgia (low-defect kaolinite) at $\rho_{b,d} = 1.67$ Mg/m^3, 25 °C and in contact with pure water. The present value for KGa-2 from Georgia (high-defect kaolinite) at 20 °C and in contact with water is $D_e = (1.33 \pm 0.15) \times 10^{-10}$ m^2/s. The two results are in good agreement; the slightly lower value from the present experiment can be explained by the higher degree of compaction and the different type of kaolinite.

5.3. Temperature dependency

The activation energies, E_a, found in the experiments (Tables 4–8) vary between 13 and 20 kJ/mol, which is not very different (less than 25%) compared to that of the bulk water of about 17 ± 1 kJ/mol (Low, 1962; Wang, 1951). Considering the large differences in the structure between the different clays, it is concluded that the activation energy is not a very sensitive parameter for the clays under study. Nevertheless, the differences in E_a and thus of the temperature dependence of diffusion, seem to be related to specific properties of the clays.

In order to facilitate the discussion of the temperature dependence, the normalized effective diffusion coefficients for all materials and for bulk water are plotted in Fig. 5 (assuming $E_a = 17 \pm 1$ kJ/mol). The normalization was done for each clay by dividing the D_e values at the different temperatures by the value obtained at the highest common temperature, which is 60 °C, in the this case. In this way, one eliminates the influence of the macroscopic geometry parameters like porosity and tortuosity (provided they indeed remained constant for all temperatures). Using the value at the highest common temperature for the normalization is based on the idea that the higher the temperature (and thus the higher the thermal energy of the water molecules), the smaller are the effects imposed on diffusion by the physical and chemical interactions with the clay surfaces and cations. In contrast, for lower temperatures the effects of these interactions are expected to become more important.

As shown in Fig. 5 for the samples saturated at high ionic strength, the normalized values of the montmorillonites fall below those of bulk water with decreasing temperatures, indicating that there the interactions of the water with the interlayer surfaces additionally impede diffusion. In contrast, the normalized Na-illite and kaolinite values remain above those of bulk water for lower temperatures, meaning that the diffusion is accelerated by inter-

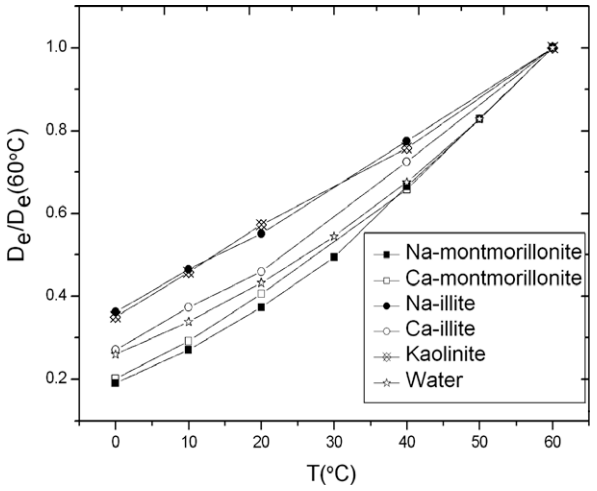

Fig. 5. Normalized effective diffusion coefficients at 1 M NaCl (Na-montmorillonite, Na-illite and kaolinite), and at 0.5 M $CaCl_2$ (Ca-clay forms). The diffusion coefficients were normalized to D_e measured at 60 °C.

actions with the cations and the external surfaces of these clays compared to bulk water. The Ca-illite values remain closer to the normalized water values. Obviously, for the external surfaces of illite, the type of cation (Na or Ca) clearly affects the interaction with the water molecules. In summary, swelling clays like montmorillonite interact strongly with the water and reduce its diffusive mobility at low temperatures compared to bulk water, whereas non-swelling clays either have small effect (Ca-illite) or even increase (Na-illite, kaolinite) the diffusive mobility of the pore water. Similar conclusions can also be determined for the samples saturated at low ionic strength. In the following, the temperature dependence of diffusion for each clay will be discussed in more detail.

The activation energies obtained for **Na- and Ca-montmorillonite** were similar, ~20 kJ/mol, and higher than the one obtained for bulk liquid water in the same temperature range. Nakazawa et al. (1999) and Suzuki et al. (2004) found similar results (E_a = 18 ± 2 kJ/mol) for Na-montmorillonite (Kunipia-F) at the same degree of compaction (where most of the water is located in the interlayer space). Most of the E_a values found in the literature for macroscopic water self-diffusion or ion diffusion in compacted clays are similar to or higher than those of bulk water (e.g., for the diffusion of Na^+ ions E_a = 24.7 ± 1.5 kJ/mol; Kozaki et al., 2005). Authors always attribute these higher values to the interactions with surfaces and the effect caused by the hydration of cations. Water in the interlayers is considered as partly bound and ordered around the Na or Ca cation (Ichikawa et al., 1999; Kawamura and Ichikawa, 2001), both order-makers. Accordingly, more energy would be required for the water molecules to break bonds to adjacent water molecules, ions or clay sites and to displace other water molecules or ions in moving from one equilibrium position to the next (Suzuki et al., 2004). Such an explanation seems plausible in the present case as well, but other reasons cannot be excluded, such as a rearrangement of the clay particles caused by the increase of temperature (especially for clays with a strong swelling behavior). This change of the particle geometry may reduce the tortuosity. Ignoring this change of tortuosity would result erroneously in an increased (or decreased) activation energy.

The activation energies for the **illites** are lower than those for the montmorillonites, but the difference between the Na- and the Ca-form is larger (Na-illite ~13 kJ/mol, Ca-illite ~16 kJ/mol). For these materials, no published E_a values were found for comparison. Both illites have lower values than that of bulk water. As for the diffusion coefficients, the differences in E_a for the two forms of illite point to the importance of the water-cation interaction. The larger value of E_a for the Ca-form would be consistent with the fact that Ca^{2+} has a stronger kosmotropic character than Na^+.

Kaolinite has an E_a value of about 14–15 kJ/mol, which is also lower than that of bulk water. Similarly to the illites, the kaolinite surfaces may disturb the water structure. However, the kaolinite samples contain mainly bulk water (average number of water molecules between surfaces of 20), so one would not expect a dominating effect by the surfaces unless the water properties close to surfaces would be strongly altered. Jonas et al. (1982) and Fripiat et al. (1984) investigated the water dynamics in kaolinite suspensions, KGa-1, close to its surface at different pressures with NMR. The activation energy of water for rotational movements was extremely reduced compared to that of bulk water. From these data it can be concluded that the kaolinite surfaces effectively change the well developed H bond network of the water in the vicinity of the surfaces, especially at low temperatures. Moreover, kaolinite is considered to have a hydrophobic (tetrahedra) and hydrophylic (octahedra) side (Tunega et al., 2002). Hydrophobic pores were found by molecular dynamic studies to accelerate water diffusion, especially at low temperatures (Hartnig et al., 1998). At high temperatures the effects would be minor, because the thermal agitation energy may outweight the interactions between water and clay surfaces, which would result in a decrease of the activation energy.

6. Summary and conclusions

The dynamics of water in 5 water saturated, and compacted clays was determined at a macroscopic scale by means of tracer through-diffusion experiments as a function of temperature and ionic strength.

No significant differences in the effective diffusion coefficients between the 2 or 4 different ionic strengths studied were found for the investigated clays at $\rho_{b,d}$ = 1.90 ± 0.05 Mg/m^3. However the systematic structural differences between the clays clearly affected water diffusion. The lowest effective diffusion coefficients (those found for Na- and Ca-montmorillonite) correspond to the highest activation energies. The effective diffusion coefficient of Ca-montmorillonite was 60% higher than that of the Na-form. This difference is interpreted as arising mainly from geometrical factors; that is, different sizes and arrangements of the particles. Sodium-montmorillonite has fewer layers per stack and smaller particles, which results in a more tortuous diffusion path than that for Ca-montmorillonite. No difference was found in the E_a between these two montmorillonite forms, which supports the interpretation that D_e differences are mostly caused by geometrical effects. In illite the effect of cations on the effective diffusion coefficients is opposite to that found in montmorillonite, but the difference is relatively small. This difference can possibly be explained by the stronger hydration energy and the stronger order-making character of Ca^{2+} compared with Na^+. This fact is also visible in the activation energy results, with E_a being higher for Ca-illite than for Na-illite. Geometrical effects are discarded here because the particle arrangement and size are very similar for these two clays. Kaolinite and both illites activation energies are lower than those of bulk water. This could be caused by the disturbance of the structure of water by these clay surfaces, which may weaken the average H-bonding of the water molecules.

The interpretations of the measured activation energies for water diffusion cannot in all cases be supported by independent evidence. Nevertheless, it seems that the observations can be linked to the specific structural (fabric) properties of the different clays.

Acknowledgements

The authors would like to acknowledge W. Müller and J. López Dólera for support in the laboratory. Additional thanks go to B. Baeyens and U. Berner for many helpful comments and to P. Blair for help with the computer. We are also thankful to R. Zurbriggen (Elotex Company) for making available the zeta-sizer instrument. This project was partially financed by the National Cooperative for the disposal of radioactive waste (NAGRA), Wettingen, Switzerland.

References

Bourg, I.C., Sposito, G., Bourg, A.C.M., 2006. Tracer diffusion in compacted, water-saturated bentonite. Clays Clay Miner. 54, 363–374.

Boving, T.B., Grathwohl, P., 2001. Tracer diffusion coefficients in sedimentary rocks: correlation to porosity and hydraulic conductivity. J. Contam. Hydrol. 53, 85–100.

Bridgeman, C.H., Skipper, N.T., 1997. A Monte Carlo study of water at an uncharged clay surface. J. Phys.: Condens. Matter 9, 4081–4087.

Bucher, F., Spiegel, U., 1984. Quelldruck von Hochverdichteten Bentoniten. Nagra Technical report NTB 84-18. Nagra, Wettingen, Switzerland.

Choi, J.W., Oscarson, D.W., 1996. Diffusive transport through compacted Na- and Ca-bentonite. J. Contam. Hydrol. 22, 189–202.

Chorover, J., Amistadi, M.K., Burgos, W.D., Hatcher, P.G., 1999. Quinoline sorption on kaolinite-humic acid complexes. Soil Sci. Soc. Am. J. 63, 850–857.

Decher, A., 1997. Bentonite der Insel Milos, Griechenland, T.H. Aachen, Germany. Doctoral thesis. ISBN: 3-86073-602-7.

Dill, K.A., Truskett, T.M., Vlachy, V., Hribar-Lee, B., 2005. Modeling water, the hydrophobic effect, and ion solvation. Ann. Rev. Biophys. Biomol. Struct. 34, 173–199.

Djeran-Maigre, I., Tessier, D., Grunberger, D., Velde, B., Vasseur, G., 1998. Evolution of microstructures and of macroscopic properties of some clays during experimental compaction. Mar. Petrol. Geol. 15, 109–128.

Ellis, J.H., Barnhisel, R.I., Phillips, R.E., 1970. The diffusion of copper, manganese, and zinc as affected by concentration, clay mineralogy, and associated anions. Soil. Sci. Soc. Am. Proc. 34, 866–870.

Fernández, A.M., 2003. Characterización y modelización del agua intersticial de materiales arcillosos: estudio de la bentonita del Cortijo de Archidona. Departamento de Química Agrícola, Geología y Geoquímica. Univ. Autónoma de Madrid. Doctoral thesis.

Flury, M., Gimmi, T., 2002. Solute diffusion. In: Topp, J.H.D.a.G.C. (Ed.), Methods of Soil Analysis, Part 4—Physical Methods. Soil Science Society of America Inc., Madison, Wisconsin, USA, pp. 323–1351.

Fripiat, J.J., Letellier, M., Levitz, P., 1984. Interaction of Water with Clay Surfaces. Philos. Trans. R. Soc. London Series A—Math. Phys. Eng. Sci. 311, 287.

Gabis, V., 1958. Etude préliminaire des argiles oligocènes du Puy-en-Velay (Haute-Loire). Bull. Soc. Franç. Minéral. Cristallog. 81, 183–185.

García-Gutiérrez, M., Mingarro, M., Missana, T., Martin, P.L., Sedano, L.A., Cormenzana, J.L., 2004. Diffusion experiments with compacted powder/pellets clay mixtures. Appl. Clay Sci. 26, 57–64.

Gast, R.G., 1962. An interpretation of self-diffusion measurements of cations in clay water systems. J. Colloid Sci. 17, 492–500.

Glaus, M.A., Baeyens, B., Bradbury, M.H., Jakob, A., Van Loon, L.R., Yaroshchuk, A., 2007. Diffusion of Na-22 and Sr-85 in montmorillonite: Evidence of interlayer diffusion being the dominant pathway at high compaction. Environ. Sci. Technol. 41, 478–485.

Hartnig, C., Witschel, W., Spohr, E., 1998. Molecular dynamics study of the structure and dynamics of water in cylindrical pores. J. Phys. Chem. B 102, 1241–1249.

Hassan, M.S., Villieras, F., Gaboriaud, F., Razafitianamaharavo, A., 2006. AFM and low-pressure argon adsorption analysis of geometrical properties of phyllosilicates. J. Colloid Interface Sci. 296, 614–623.

Hribar, B., Southall, N.T., Vlachy, V., Dill, K.A., 2002. How ions affect the structure of water. J. Am. Chem. Soc. 124, 12302–12311.

Ichikawa, Y., Kawamura, K., Nakano, M., Kitayama, K., Kawamura, H., 1999. Unified molecular dynamics and homogenization analysis for bentonite behavior: current results and future possibilities. Eng. Geol. 54, 21–31.

Jonas, J., Brown, D., Fripiat, J.J., 1982. NMR Study of Kaolinite-Water System at High Pressure. J. Colloid Interface Sci. 89, 374–377.

Kawamura, K., Ichikawa, Y., 2001. Physical properties of clay minerals and water—by means of molecular dynamics simulations. Bull. Earthquake Res. Inst., Univ. Tokyo 76, 311–320.

Kozaki, T., Fujishima, A., Sato, S., Ohashi, H., 1998. Self-diffusion of sodium ions in compacted sodium montmorillonite. Nucl. Technol. 121, 63–69.

Kozaki, T., Fujishima, A., Saito, N., Sato, S., Ohashi, H., 2005. Effects of dry density and exchangeable cations on the diffusion process of sodium ions in compacted montmorillonite. Eng. Geol. 81, 246–254.

Kozaki, T., Sato, Y., Nakajima, M., Kato, H., Sato, S., Ohashi, H., 1999. Effect of particle size on the diffusion behavior of some radionuclides in compacted bentonite. J. Nucl. Mater. 270, 265–272.

Li, Y., Gregory, S., 1974. Diffusion of ions in sea water and in deep-sea sediments. Geochim Cosmochim. Acta 38, 703–714.

Low, P.F., 1962. Influence of absorbed water on exchangeable ion movement. Clays Clay Miner. 9, 219–228.

Marra, J., 1986. Effects of Counterion Specificity on the Interactions between Quaternary Ammonium Surfactants in Monolayers and Bilayers. J. Phys. Chem. 90, 2145–2150.

Marry, V., Turq, P., 2003. Microscopic simulations of interlayer structure and dynamics in bihydrated heteroionic montmorillonites. J. Phys. Chem. B 107, 1832–1839.

McBride, M.B., 1994. Environmental Chemistry of Soils. Oxford University Press.

Melkior, T., Yahiaoui, S., Motellier, S., Thoby, D., Tevissen, E., 2005. Cesium sorption and diffusion in Bure mudrock samples. Appl. Clay Sci. 29, 172–186.

Mellor, J.D., 1978. Fundamental of Freeze-Drying. Academic Press, London, NY.

Nakazawa, T., Takano, M., Nobuhara, A., Torikai, Y., Sato, S., Ohashi, H., 1999. Activation energies of diffusion of tritium and electrical conduction in water-saturated compacted sodium montmorillonite. In: Proc. Radioactive Waste Management and Environmental Remediation. ASME.

Ohtaki, H., Radnai, T., 1993. Structure and Dynamics of Hydrated Ions. Chem. Rev. 93, 1157–1204.

Oster, J.D., Low, P.F., 1963. Activation energy for ion movement in thin water films on montmorillonite. Soil Sci. Soc. Am. Proc. 27, 369–373.

Phillips, R.E., Brown, D.A., 1968. Self-diffusion of tritiated water in Montmorillonite and kaolinite clay. Soil Sci. Soc. Am. Proc. 32, 302–306.

Poinssot, C., Baeyens, B., Bradbury, M.H., 1999. Experimental studies of Cs, Sr, Ni, and Eu sorption on Na-illite and the modelling of Cs sorption. PSI Technical report. ISSN 1019-0643. Paul Scherrer Institute, PSI, Villigen, Switzerland.

Pusch, R., 2001. The microestructure of MX-80 clay with respect to its bulk physical properties under different enviromental conditions. SKB Technical report. Swedish Nuclear Fuel and Waste Management Co. (SKB). ISSN 1404-0344.

Sachs, S., Křepelová, A., Schmeide, K., Koban, A., Günther, A., Mibus, J., Brendler, V., Geipel, G., Bernhard, G., 2006. Joint project: Migration of actinides in the system clay, humic substance, aquifer – migration behavior of actinides (uranium, neptunium) in clays: Characterization and quantification of the influence of humic substances. Technical report. Forschungszentrum Dresden-Rossendorf, Institut für Radiochemie, Dresden, Germany. ISSN 1437-322X.

Sato, H., 2002. A study on the effect of clay particle orientation on diffusion in compacted bentonite. In: Tucson, A.Z. (Ed.), Proc. WM'02 Conf., F-, 2002, WM'02 Conf. Tucson, AZ.

Slowinski, E.J., Wolsey, W.C., Masterton, W.L., 2004. Chemical Principles in the Laboratory, eighth ed., Brooks/Cole, T.

Sposito, G., Prost, R., 1982. Structure of Water Adsorbed on Smectites. Chem. Rev. 82, 553–573.

Suzuki, S., Sato, H., Ishidera, T., Fujii, N., 2004. Study on anisotropy of effective diffusion coefficient and activation energy for deuterated water in compacted sodium bentonite. J. Contam. Hydrol. 68, 23–37.

Tunega, D., Benco, L., Haberhauer, G., Gerzabek, M.H., Lischka, H., 2002. Ab initio molecular dynamics study of adsorption sites on the (001) surfaces of 1:1 dioctahedral clay minerals. J. Phys. Chem. B 106, 11515–11525.

van Brakel, J., Heertjes, P.M., 1974. Analysis of diffusion in macroporous media in terms of porosity, tortuosity and constrictivity factor. Int. J. Heat Mass Transfer 17, 1093–1103.

Van Loon, L.R., Muller, W., Iijima, K., 2005. Activation energies of the self-diffusion of HTO, ^{22}Na and ^{36}Cl in a highly compacted argillaceous rock (Opalinus Clay). Appl. Geochem. 20, 961–972.

Van Loon, L.R., Soler, J.M., Jakob, A., Bradbury, M.H., 2003. Effect of confining pressure on the diffusion of HTO, ^{36}Cl and ^{125}I in a layered argillaceous rock (Opalinus Clay): diffusion perpendicular to the fabric. Appl. Geochem. 18, 1653–1662.

Van Loon, L.R., Soler, J.M., Muller, W., Bradbury, M.H., 2004. Anisotropic diffusion in layered argillaceous rocks: a case study with opalinus clay. Environ. Sci. Technol. 38, 5721–5728.

van Olphen, H., 1966. An Introduction to Clay Colloid Chemistry: For Clay Technologists, Geologists, and Soil Scientists. I. Houston, Texas.

van Olphen, H., Fripiat, J.J., 1979. Data Hand Book for Clay Minerals, ISBN-0-08-022850-0-X.

Vasseur, G., Djeranmaigre, I., Grunberger, D., Rousset, G., Tessier, D., Velde, B., 1995. Evolution of structural and physical parameters of clays during experimental compaction. Mar. Petrol. Geol. 12, 941–954.

Wang, J.H., 1951. Self-diffusion and structure of liquid water .1. measurement of self-diffusion of liquid water with deuterium as tracer.. J. Am. Chem. Soc. 73, 510–513.

Wang, J.H., 1954. Effect of ions on the self-diffusion and structure of water in aqueous electrolytic solutions. J. Phys. Chem. 58, 686–692.

Wang, Y.H., Siu, W.K., 2006. Structure characteristics and mechanical properties of kaolinite soils I. Surface charges and structural characterizations. Can. Geotech. J. 43, 587–600.

Wu, T.C., Bassett, W.A., Huang, W.L., Guggenheim, S., vanGroos, A.F.K., 1997. Montmorillonite under high H2O pressures: Stability of hydrate phases, rehydration hysteresis, and the effect of interlayer cations. Am. Mineral. 82, 69–78.

Yong, R.N., 2003. Influence of microstructural features on water, ion diffusion and transport in clay soils. Appl. Clay Sci. 23, 3–13.